Editors' Suggestion

Expediting viscous spreading with liquid-infused solids

Saurabh Nath and David Quéré
Physique et Mécanique des Milieux Hétérogènes, UMR 7636 du CNRS, PSL Research University, ESPCI, 75005 Paris, France

(Received 19 July 2022; revised 12 January 2023; accepted 12 March 2024; published 6 May 2024)

Here we discuss how the use of textured liquid-infused solids can expedite the dynamics of spreading of viscous drops, when the subjacent oil layer is less viscous. We characterize the nature and amplitude of the effect, and the laws governing the spreading at short time. More generally, our findings affirm the universality of the early dynamics of viscous contact, found to hold for drops that coalesce, spread, or even, like here, slip on their substrate.

DOI: 10.1103/PhysRevFluids.9.054001

I. INTRODUCTION

Viscous drops on a solid spread slower and slower until they reach their equilibrium, which, generally, consists of a lens meeting the solid with a finite contact angle [1]. We wonder here if we can take advantage of the slippery character of the so-called liquid-infused solids (LIS) [2,3] to speed up the process and reach equilibrium in a reduced time. Implementing slip at a solid-liquid interface should generally favor the dynamics. However, LIS are also known to induce additional sources of friction such as that associated with the oil meniscus that forms around deposited drops [4–6], which makes the question nontrivial. For instance, water drops spreading on viscous infused solids were observed to spread slower than on regular solids, owing to the supplemental dissipation in the subjacent oil film [7].

The fate of drops touching a flat surface is often decided by their short time behaviors—for instance, in soldering, where drops solidify right after contact [8], or more generally when non-viscous liquids partially wet the solid and find their final state in a few milliseconds. However, while the dynamics of spreading have been studied for more than half a century, its first steps were only discussed in the last two decades [9–13]. For drops with surface tension γ, density ρ, viscosity η, and radius R, the main conclusions of these researches can be summarized as follows: (i) the contact radius r of a droplet with low viscosity ($\eta < 10$ mPa s) grows with a diffusive-type law $r \sim R(t/\tau_0)^{1/2}$, where $\tau_0 = (\rho R^3/\gamma)^{1/2}$ is the inertia-capillary time of the drop [6,9,10]; (ii) conversely, the contact of a viscous drop ($\eta > 10$ mPa s) follows the dynamics $r \sim R(t/\tau)\ln(\tau/t)$, where $\tau = \eta R/\gamma$ is the visco-capillary time of the drop [13]. This law, further referred to as the ELS law, was first proposed by Eggers, Lister, and Stone in the context of drop coalescence [14] and generalized here to spreading. Remarkably, this behavior does not obey a scaling law in time, a unique feature in wetting dynamics. At very short time, it is slower than the inertial dynamics, which justifies why it should kinetically take the lead. However, the law does not include any information about the substrate, and we discuss here how (or whether) a slippery material might modify it.

II. MATERIALS

Spreading dynamics are tested by making a 1 μl drop of glycerol contact either a solid or a LIS, that is, a textured solid infused with oil. Oil is chosen such that glycerol remains on the top of the wet texture and its viscosity at most matches that of glycerol, so that it can remain mobile as the viscous liquid atop spreads [5]. This case opposes that of [7], where low viscosity drops were found to be slowed down by the presence of a viscous infusion. For studying the dynamics, side views are difficult to exploit because of the cusplike nature of contact. We would rather use transparent substrates, allowing us to image spreading from the top. Transparent hydrophobic solids are made by exposing a glass slide to oxygen plasma for 5 min and then functionalizing it with trichloro(1H, 1H, 2H, 2H-perfluoro-octyl)silane (Sigma-Aldrich) through vapor deposition for 30 min. The contact angle of glycerol on this surface is around 90°, comparable to its apparent angle on a LIS infused with silicone oil.

In order to prepare the liquid-infused surfaces, we first spin-coat SU-8 resin on a silicon wafer and then shine UV light through a mask to get a square array of circular pillars. Using a polydimethylsiloxane countermold of this sample, we eventually get a transparent texture made of optical adhesive (Norland Optical Adhesive) on a glass slide, with pillars with height $h = 20 \pm 3$ μm, lateral size $d = 18$ μm, and spacing $p = 15$ μm of density, thus of density $\phi = 23\%$–25% (ratio of pillar top area to the total area). We finally add a second scale of roughness, by drawing the microtextured substrate from a solution of hydrophobic nanobeads (Glaco Mirror Coat, Soft 99) [15]. After evaporating the solvent at 70 °C for 30 min, the beads (∼30 nm) coat both the substrate and the pillars without altering transparency. The process is repeated three times to ensure uniformity of the coating.

We infuse the textured solid with silicone oil of viscosity η_0 between 5 and 970 mPa s. The optical index of the oil is comparable to that of the resin, which enhances the transparency of the material. Infusion is performed by bringing the vertical substrate in contact with the reservoir of silicone oil that wicks in only within the texture, without overinfusing. Oil penetrates both between the pillars and within the nanobead cavities, which minimizes the pinning of glycerol on the pillar edges and tops (roll-off angle of $\sim 1^\circ$ for 20 μl drops).

III. EXPERIMENTS

As sketched in Fig. 1, a glycerol drop is first placed on a Glaco-treated, superhydrophobic glass slide, which maintains its sphericity. Then we approach the drop with the substrate from the top, at a low speed (about 50 μm/s). This method avoids impact (and its specific spreading dynamics), as would happen if drops were released above the materials. We image spreading with a high-speed camera with 20–70 000 frames per second. The experiment is repeated multiple times for droplet volumes of 1 and 4 μl and for seven oil viscosities, namely, 5, 9, 19, 48, 96, 485, and 970 mPa s. Another experiment is done with the same setup, replacing the LIS by a hydrophobic glass, so that we can extract the original contribution of infusion in the contact dynamics.

Figure 1 compares the evolution of the solid-liquid contact of a 1 μl glycerol drop on a hydrophobic solid (bottom row) and on a LIS with oil viscosity varying between 9 and 970 mPa s (from top to bottom). The drop appears in black, except the contact area where backlighting provides light. It seems from the images that the contact size roughly grows linearly in time, with a typical velocity function of the oil viscosity: as η_0 increases, spreading gets visibly slower, by a factor of 2–3. In addition, its kinetics becomes comparable to that on a solid when the oil viscosity is similar to that of glycerol (around 1000 mPa s). Hence, a nonviscous oil significantly accelerates the spreading of a viscous liquid, showing that a LIS can be slippery not only from the adhesion point of view, but also from a frictional perspective. This result contrasts with previous observations made with water, for which LIS were rather observed to be a strong source of supplementary friction [4–7].

These observations can be made more quantitative by plotting the time evolution of the contact radius r. We report it in Figs. 2(a) and 2(b) for a 1 μl glycerol drop and all tested substrates, from

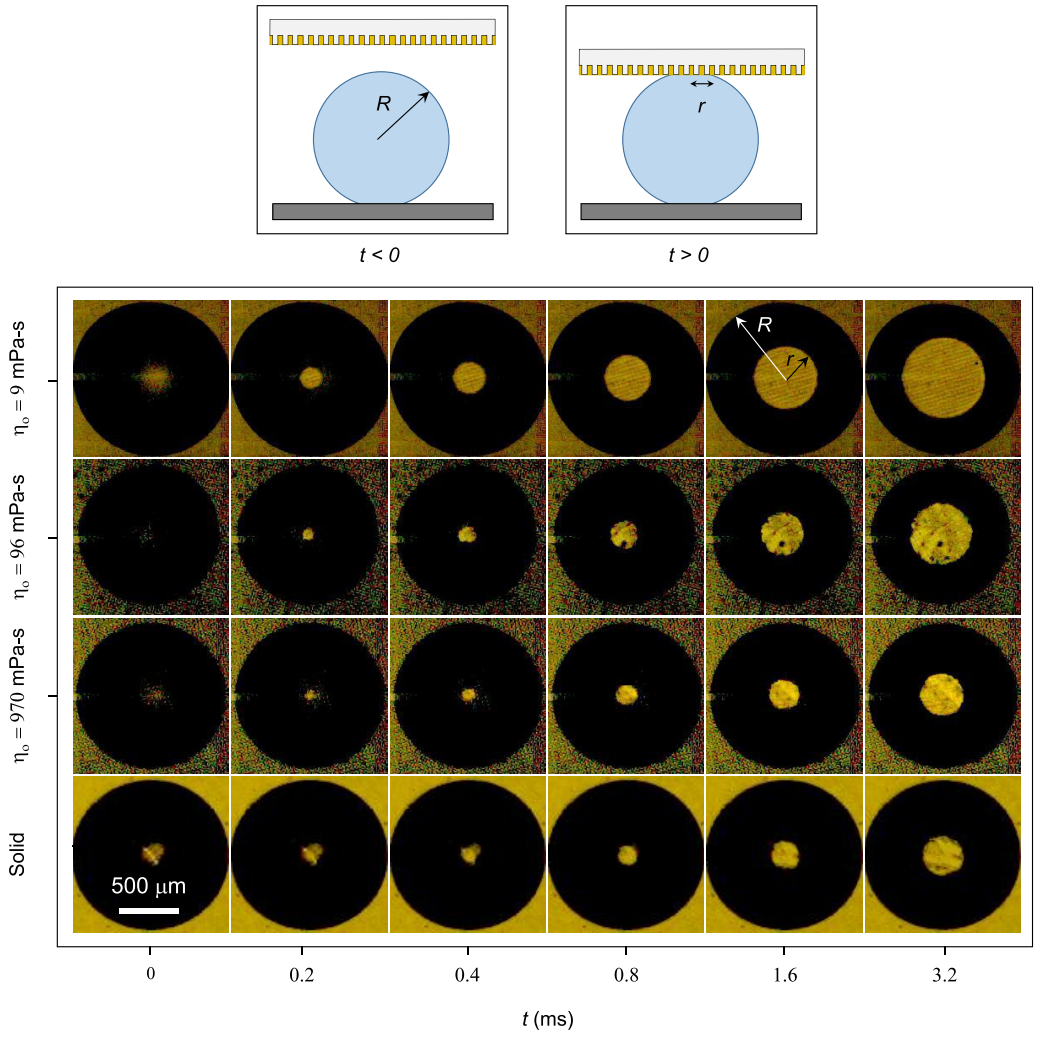

FIG. 1. Top: Schematic of a glycerol drop with radius R brought in contact (at $t = 0$) with a transparent infused surface. Down: Top-view time lapse of 1 μl glycerol droplets spreading on a transparent LIS for oil viscosities $\eta_0 = 9$ mPa s, $\eta_0 = 96$ mPa s, and $\eta_o = 970$ mPa s, or on a hydrophobic glass slide (down row). We note that the contact, with radius r and orange in the photos, propagates faster when the solid is infused; the lower the oil viscosity, the faster the wetting. For a more complete series of oil viscosities, see the Supplemental Material movie.

the hydrophobic solid to LIS with viscosity varied by a factor of 200. The plot confirms the trends seen in Fig. 1: the lower the oil viscosity, the faster the spreading, an effect that leads to substantial reduction in the spreading time. As seen in Fig. 2(c), the time τ_r needed to reach a given radius r is decreased by a factor ∼4 when reducing the oil viscosity by two orders of magnitude.

Remarkably, all dynamics of spreading can be fitted by the ELS law, $r = A(\gamma t/\eta)\ln(R/r)$, shown with solid lines in Fig. 2(a) (see also the Supplemental Material for separate plots [16]), whatever the substrate, solid or infused. Varying the oil viscosity just shifts the data. Oil at the interface between glycerol and the substrate might provide slip and affect coefficients, but not the law itself. If we assume that the boundary condition at the LIS-glycerol interface is reflected by a renormalization of the viscosity η, we can first qualitatively consider that glycerol spreads with an effective viscosity

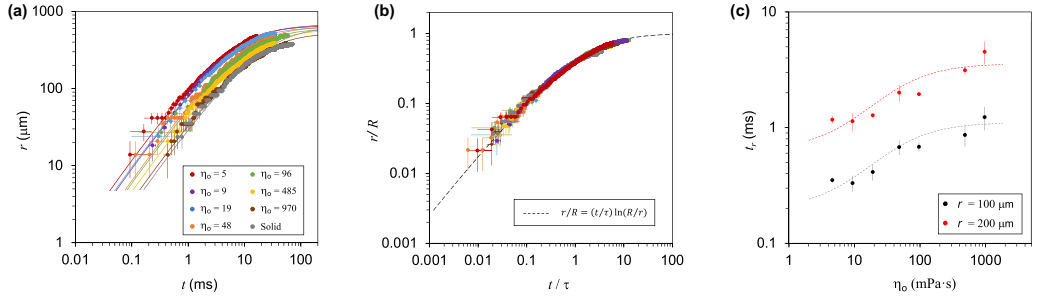

FIG. 2. (a) Contact radius r between a glycerol drop (volume 1 μl) and its substrate, as a function of time t, either on a hydrophobic solid (gray data), or on a LIS with $\eta_0 = 5$ mPa s (red), 9 mPa s (purple), 19 mPa s (blue), 48 mPa s (orange), 96 mPa s (green), 485 mPa s (yellow), and 970 mPa s (brown). Solid lines show the ELS law (introduced in the text), $r = A(\gamma t/\eta)\ln(R/r)$, where A is a prefactor treated as an adjustable parameter in the fits. Its value is found to vary with the oil viscosity. (b) The same data collapse after normalizing r by the drop radius R, and t by the visco-capillary time $\tau = \eta R/A\gamma$ of glycerol including the parameter A. (c) Time τ_r observed to reach a given radius $r = 100$ μm (black data) or $r = 200$ μm (red data). Both plots exhibit the same trend and show that spreading is accelerated by a factor ~ 4 when the oil viscosity falls from 970 to 5 mPa s.

η/A, where A is an increasing function of slip. This intuitive approach is confirmed after normalizing r by the drop radius R and t by the time $\eta R/A\gamma$: as seen in Fig. 2(b), data then collapse on a single ELS curve (dashed line).

IV. DISCUSSION

The ELS law of contact is thus observed to resist a change in the boundary conditions—be it the classical no slip on a "bare" solid, or slip on the LIS. The latter, we note, is along the vein of the coalescence of two drops [14,17], the original frame of ELS law [14]. Considering the complexity of the system, it is useful to first rederive the ELS law for a spreading liquid, using a poor man's approach.

As sketched in Fig. 3(a), the propagation of liquid evacuates the air initially present below the drop and we assume the tip of the solid-liquid contact region to be rounded by surface tension. The height δ of this gap is given by geometry, $\delta \sim r^2/R$, and we shall adopt this simple view to derive the contact dynamics—even if slightly more complex profiles of the interface can be considered, with the existence of a rim, for instance, when the air viscosity needs to be considered [14].

As the solid-liquid contact propagates, viscous dissipation takes place in a toroidal region of perimeter $2\pi r$ and height of order δ, with a corresponding Stokes friction per unit length $F \sim \eta V/\ln(2\pi r/\delta)$. Balancing it with the driving surface tension, of order γ, we get a contact velocity $V \sim (\gamma/\eta)\ln(r/\delta) \sim (\gamma/\eta)\ln(R/r)$, where we recognize the ELS law [14]. Integrating over time for $r/R \ll 1$, we deduce a contact dynamics $r \sim (\gamma/\eta)t\ln(R/r)$, a pseudolinear law distorted by a logarithmic correction [18]. If we introduce the numerical factor A missing in the scaling argument, we obtain $r = A(\gamma t/\eta)\ln(R/r)$, the function fitting the data in Figs. 2(a) and 2(b). Expanding it at short time provides an explicit form for the contact evolution, $r \sim R(t/\tau)\ln(\tau/t)$, with $\tau = A\eta R/\gamma$, which justifies the scaling of time in Fig. 2(b).

The fitting coefficients A deduced from Fig. 2(a) are reported in Fig. 3(b) as a function of the oil viscosity η_0 normalized by the glycerol viscosity η. A directly quantifies how the use of a nonviscous oil expedites the spreading of glycerol. Assuming that the effect arises from slip at the substrate-drop interface, A can be seen as a slip factor that increases from ~ 1 to ~ 4 when oil becomes less viscous. We also note that the value of A at high η_0 is comparable to that on a solid ($A = 0.7 \pm 0.1$ on our

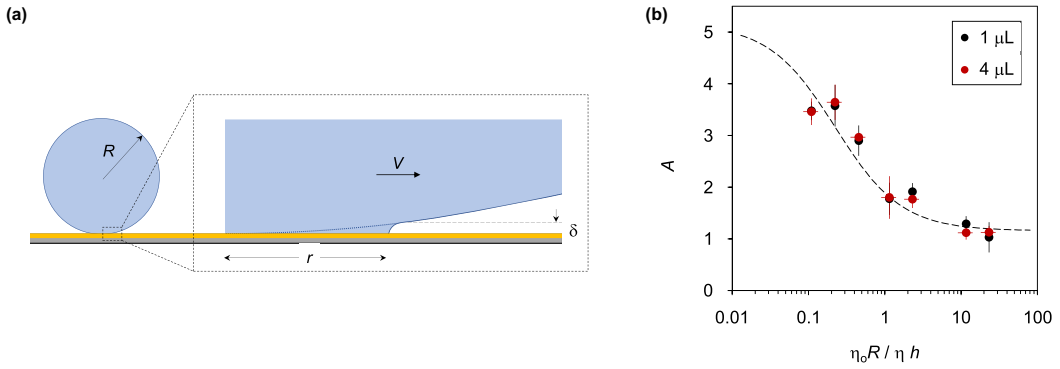

FIG. 3. (a) Schematic of a viscous drop (in blue) contacting a flat substrate. Inset shows the initial profile of the drop (dotted line), and the profile after the solid-liquid contact has propagated by a distance r at a velocity V (full line). The characteristic height of the region close to the contact line is denoted as δ. (b) The slip factor A extracted from the fits in Fig. 2(a) is plotted as a function of the ratio $\eta_0 R/\eta h$ for glycerol drops (1 μl, black data and 4 μl, red data) spreading on a LIS with $h = 20$ μm and infused with oil of viscosity between 5 and 970 mPa s. The dashed line shows the behavior expected from the model.

hydrophobic solid, $A = 1.0 \pm 0.1$ on a hydrophilic one [13]) and that slip logically vanishes when oil and glycerol have similar viscosities.

The factor A on a solid is significantly larger than $1/4\pi$, the coefficient calculated for coalescing viscous drops [14]. On a solid, we expect supplementary friction at the solid-liquid interface. For a contact angle around 90°, we assume that the contact line friction, most often dominant for acute angles, is negligible compared to the Stokes friction in the toroidal region where glycerol is injected as the drop spreads. This provides a force with the same scaling as previously, but with a different coefficient, due to the presence of the solid, making us realize why ELS law can still hold as a viscous drop "coalesces" with a solid.

In addition, slip can exist at the LIS-glycerol interface, which decreases the interfacial friction in proportion to the degree of slip. Denoting V_s as the slip velocity at the interface, we propose to write the toroidal Stokes friction as the sum of a coalescence term (the only term for pure slip, $V_s = V$), $F_1 \sim \eta V/\ln(R/r)$, and of an interfacial term, $F_2 \sim \eta(V - V_s)/\ln(R/r)$. The slip velocity V_s is evaluated by balancing viscous stresses at the interface, $\eta(V - V_s)/R \sim \eta_0 V_s/h$. This yields $V - V_s \sim KV$, where the number $K = \eta_0 R/(\eta_0 R + \eta h)$ is a function of the quantity $\eta h/\eta_0 R$ only. When the oil viscosity η_0 vanishes, so does K, and slip is maximized ($V_s \sim V$). Conversely, when the drop loses its viscosity η, K tends to 1 and we recover the classical no-slip situation ($V_s \sim 0$). Balancing the viscous force $F_1 + F_2$ with surface tension γ, we get a spreading velocity of the form derived for coalescence, $V \sim (\gamma/\eta)(1 + K)^{-1} \ln(R/r)$, where slip dictates the spreading dynamics whose speed increases as K goes from 1 (no slip) to 0 (pure slip).

We can finally introduce the numerical factors α and β missing in the scaling expressions of F_1 and F_2, which yields a slip factor $A = (\alpha + \beta K)^{-1}$. In Fig. 3(b), we plot the values of A deduced from Fig. 2(a) as a function of the number $\eta_0 R/\eta h$, and we compare the data with the model (dashed line) drawn for $h = 20$ μm and for the volumes we tested (1 and 4 μl). The agreement is good for $\alpha = 0.19 \pm 0.04$ and $\beta = 0.7 \pm 0.1$, two values that remain to be understood. More broadly, the model explains why all data can be fitted by ELS law. Changing the material, from solid to viscous LIS, and from viscous LIS to slippery LIS, just impacts the prefactor A. As seen in Fig. 3(b), the value of A and thus the dynamics varies between two plateaus: as the oil viscosity increases, we switch from a pure-slip situation that maximizes the speed of wetting ($A = 1/\alpha$), to a no-slip condition that minimizes it [$A = 1/(\alpha + \beta)$]. According to the model, the slip effect could also be activated by increasing the pillar height—showing that the two main characteristics of a LIS (where

the oil nature and the pillar geometry can be tuned independently) may be actuated to speed up the spreading of viscous liquids.

The ELS law has to transition to a subsequent inertial law, $r \sim R(t/\tau_0)^{1/2}$ with $\tau_0 = (\rho R^3/\gamma)^{1/2}$, and we wonder here when this transition occurs. Comparing both laws shows that inertia dominates when the contact size verifies the inequality $r/R \ \ln(R/r) > \mathrm{Oh}$, where $\mathrm{Oh} = \eta/\sqrt{\rho\gamma R}$ is the Ohnesorge number. For a millimetric drop of water ($\mathrm{Oh} \approx 4 \times 10^{-3}$), the inertial regime should be observed for $r \gtrsim 0.1$ μm, that is, from a microscopic scale, which explains why the viscous regime was not reported for the early spreading of water [9]. Conversely, inertia should always be negligible for glycerol (Oh≈4), which justifies why we do not report the corresponding regime; the viscous law then either lasts until a stop in partial wetting (our case), or switches to the classical Tanner's regime ($r \sim t^{1/10}$) in complete wetting [19]. It would be worth testing the spreading of liquids with intermediate viscosity, a case where we expect a crossover between the two early regimes of contact (ELS, inertial).

In the opposite limit of low viscosity drops (as water) on a viscous LIS, a slowing down of the spreading dynamics was observed because the oil film in the texture only adds to the dissipation [7]. Nevertheless, we find that hemi-solids preserve in all cases the scaling law of spreading at short time reported on bare solids, yet with considerable changes in the magnitude of the prefactors. A natural extension of our observations here is to test a viscous drop as glycerol spreading on a LIS infused with an even higher viscosity—a regime not investigated here.

Finally, it is interesting to note that examples of expediting wetting of a drop are rare—two such instances being the addition of "superspreading" surfactants [20] and polymeric liquids [21,22]. These examples have a very different physics from the case described here, where slip emerges from a contrast of viscosities between the drop and the infused film. Slip is a boundary condition in these flows and its variability does not impact the spreading law itself but its coefficient. This universality suggests that these ideas could be generalized to problems of similar phenomenology. For instance, a cusp forms in the region where a liquid jet impinges on a viscous bath [23], which too can be described as a Stokesian slender region, leading to quantitative predictions for the sharpness and fragility of this cusp [24,25]. As seen here, even the introduction of a third liquid (or slip) does not affect the similitude with the Stokesian cusp, but rather just leads to a renormalization of the fluid viscosity. It would be interesting to withdraw (or plunge) an infused solid from a viscous bath to create and characterize the cusp at the infused wall itself—a stationary counterpart of spreading that would help us test the limits of this analogy.

ACKNOWLEDGMENTS

We are grateful to Armelle Keiser and Philip Baumli for help in designing the samples. This project has received funding from the European Union's Horizon 2020 Research and Innovation Program under the Marie Sklodowska-Curie Grant Agreement No. 722497.

[1] P. G. de Gennes, Wetting: Statics and dynamics, Rev. Mod. Phys. **57**, 827 (1985).
[2] T. S. Wong, S. H. Kang, S. K. Tang, E. J. Smythe, B. D. Hatton, A. Grinthal, and J. Aizenberg, Bioinspired self-repairing slippery surfaces with pressure-stable omniphobicity, Nature (London) **477**, 443 (2011).
[3] A. Lafuma and D. Quéré, Slippery pre-suffused surfaces, Europhys. Lett. **96**, 56001 (2011).
[4] J. D. Smith, R. Dhiman, S. Anand, E. Reza-Garduno, R. E. Cohen, G. H. McKinley, and K. K. Varanasi, Droplet mobility on lubricant-impregnated surfaces, Soft Matter **9**, 1772 (2013).
[5] A. Keiser, L. Keiser, C. Clanet, and D. Quéré, Drop friction on liquid-infused materials, Soft Matter **13**, 6981 (2017).
[6] D. Daniel, J. V. Timonen, R. Li, S. J. Velling, and J. Aizenberg, Oleoplaning droplets on lubricated surfaces, Nat. Phys. **13**, 1020 (2017).

[7] S. Nath and D. Quéré, Spreading of water on a liquid-infused solid, Phys. Rev. Fluids **7**, 084003 (2022).
[8] S. Schiaffino and A. A. Sonin, Molten droplet deposition and solidification at low Weber numbers, Phys. Fluids **9**, 3172 (1997).
[9] A. L. Biance, C. Clanet, and D. Quéré, First steps of the spreading of a liquid droplet, Phys. Rev. E **69**, 016301 (2004).
[10] J. C. Bird, S. Mandre, and H. A. Stone, Short-time dynamics of partial wetting, Phys. Rev. Lett. **100**, 234501 (2008).
[11] K. G. Winkels, J. H. Weijs, A. Eddi, and J. H. Snoeijer, Initial spreading of low-viscosity drops on partially wetting surfaces, Phys. Rev. E **85**, 055301(R) (2012).
[12] B. B. J. Stapelbroek, H. P. Jansen, E. S. Kooij, J. H. Snoeijer, and A. Eddi, Universal spreading of water drops on complex surfaces, Soft Matter **10**, 2641 (2014).
[13] A. Eddi, K. G. Winkels, and J. H. Snoeijer, Short time dynamics of viscous drop spreading, Phys. Fluids **25**, 013102 (2013).
[14] J. Eggers, J. R. Lister, and H. A. Stone, Coalescence of liquid drops, J. Fluid Mech. **401**, 293 (1999).
[15] J. H. Guan, E. R. Gutierrez, B. Xu, D. Wood, G. McHale, R. A. L. Aguilar, and G. G. Wells, Drop transport and positioning on lubricant impregnated surfaces, Soft Matter **13**, 3404 (2017).
[16] See Supplemental Material at http://link.aps.org/supplemental/10.1103/PhysRevFluids.9.054001 for additional data.
[17] J. D. Paulsen, J. C. Burton, and S. R. Nagel, Viscous to inertial crossover in liquid drop coalescence, Phys. Rev. Lett. **106**, 114501 (2011).
[18] The left-hand side of the integration is $\int_0^x \mathrm{d}x/\ln x$, where $x = r/R$. This integral, also known as the logarithmic integral function, approaches $x/\ln x$ for small x.
[19] L. Tanner, The spreading of silicone oil drops on horizontal surface, J. Phys. D **12**, 1473 (1979).
[20] S. Zhu, W. G. Miller, L. E. Scriven, and H. T. Davis, Superspreading of water-silicone surfactant on hydrophobic surfaces, Colloids Surf., A **90**, 63 (1994).
[21] F. Brochard-Wyart, P-G. de Gennes, H. Hervert, and C. Redon, Wetting and slippage of polymer melts on semi-ideal surfaces, Langmuir **10**, 1566 (1994).
[22] J. D. McGraw, T. S. Chan, S. Maurer, T. Salez, M. Benzaquen, E. Raphaël, M. Brinkman, and K. Jacobs, Slip-mediated dewetting of polymer microdroplets, Proc. Natl. Acad. Sci. USA **113**, 1168 (2016).
[23] D. Joseph, J. Nelson, M. Renardy, and Y. Renardy, Two-dimensional cusped interfaces, J. Fluid Mech. **223**, 383 (1991).
[24] J. T. Jeong and H. K. Moffatt, Free-surface cusps associated with flow at low Reynolds number, J. Fluid Mech. **241**, 1 (1992).
[25] J. Eggers, Air entrainment through free-surface cusps, Phys. Rev. Lett. **86**, 4290 (2001).